Jann, K., Jann, B., Schmidt, M. A., & Vann, W. F. (1980) *J. Bacteriol. 143*, 1108–1115.
Kennedy, E. P., Rumley, M. K., Schulman, H., & van Golde, L. M. G. (1976) *J. Biol. Chem. 251*, 4208–4213.
Knox, K. W., & Wicken, A. J. (1973) *Bacteriol. Rev. 37*, 215–257.
Koch, H. U., & Fischer, W. (1978) *Biochemistry 17*, 5275–5281.
Lambert, P. A., Hancock, I. C., & Baddiley, J. (1977) *Biochim. Biophys. Acta 472*, 1–12.
LeCocq, J., & Ballou, C. F. (1964) *Biochemistry 3*, 976–980.
Nakano, M., & Fischer, W. (1978) *Hoppe Seyler's Z. Physiol. Chem. 359*, 1–11.
Trejo, A. G., Chittenden, G. J. F., Buchanan, J. G., & Baddiley, J. (1970) *Biochem. J. 117*, 637–639.
Trejo, A. G., Haddock, J. W., Chittenden, G. J. F., & Baddiley, J. (1971) *Biochem. J. 122*, 49–57.
Ukita, T., Bates, N. A., & Carter, H. E. (1955) *J. Biol. Chem. 216*, 867–874.
Veerkamp, H. J. (1976) *Biochim. Biophys. Acta 441*, 403–411.

Transient Kinetics of Adenosine 5′-Diphosphate and Adenosine 5′-(β,γ-Imidotriphosphate) Binding to Subfragment 1 and Actosubfragment 1†

K. M. Trybus and E. W. Taylor*

ABSTRACT: The kinetics of binding of the nonhydrolyzable nucleotides adenosine 5′-diphosphate (ADP) and adenosine 5′-(β,γ-imidotriphosphate) (AMP-PNP) to myosin subfragment 1 (SF-1) and actosubfragment 1 (acto-SF-1) were reinvestigated. The binding of these ligands to SF-1 can be described by

$$M_0 + L \overset{K_0}{\rightleftharpoons} M_0{\cdot}L \overset{k_1}{\underset{k_{-1}}{\rightleftharpoons}} M_1{\cdot}L \overset{k_2}{\underset{k_{-2}}{\rightleftharpoons}} M_{12}{\cdot}L$$

The nucleotide binds in a rapid equilibrium step (K_0), followed by two first-order fluorescence transitions with $k_1 + k_{-1} \gg k_2 + k_{-2}$. The rates and amplitudes of the fluorescence transitions are different for ADP and AMP-PNP and in turn can be distinguished from the corresponding steps involved in adenosine 5′-triphosphate (ATP) binding. The similarity in the maximum rate of the observed fluorescence signal for ADP and ATP binding to SF-1 in 0.1 M KCl is fortuitous as the maximum rates differ greatly at higher ionic strength. Under favorable conditions of high ionic strength where the amplitude of the fluorescence enhancement is large, the binding of AMP-PNP to acto-SF-1 gave a fluorescence change prior to dissociation, followed by a second fluorescence transition at the same rate as the dissociation of the proteins. Thus a conformation change precedes the nucleotide-induced dissociation of actomyosin. At least three acto-SF-1–nucleotide complexes are necessary to explain the kinetic behavior.

The reactions of nonhydrolyzable nucleotides with myosin and actomyosin have been extensively investigated particularly in terms of partial reactions, which yield information on the steps of the hydrolysis cycle. The nucleotides ADP[1] and AMP-PNP as well as pyrophosphate dissociate actomyosin, and the mechanism is expected to resemble the steps in which ATP produces dissociation prior to hydrolysis. The binding of ADP or AMP-PNP to SF-1 gives a tryptophan fluorescence signal of smaller amplitude (Bagshaw & Trentham, 1974; Bagshaw et al., 1974) and a proton burst of the same amplitude as for ATP (Bagshaw & Trentham, 1974; Koretz & Taylor, 1975; Chock, 1979; Marsh et al., 1977).

Information obtained from the binding of ADP and AMP-PNP to SF-1 was used as evidence for the assignment of rate constants in the ATPase reaction by Bagshaw & Trentham (1974):

$$M + ATP \overset{1}{\rightleftharpoons} M{\cdot}ATP \overset{2}{\rightleftharpoons} M{\cdot}ATP^* \overset{3}{\rightleftharpoons} M{\cdot}Pr^{**} \overset{4}{\rightleftharpoons} M{\cdot}ADP^* \overset{5}{\rightleftharpoons} M{\cdot}ADP \overset{6}{\rightleftharpoons} M + ADP \quad (1)$$

Asterisks refer to states of enhanced protein fluorescence, and M refers to a myosin head, or subfragment 1 (SF-1). Step 4 is rate limiting at 20 °C, and steps 5 and 6 are the reversal of ADP binding. Since the maximum rates of the fluorescence enhancement for ATP and ADP binding to SF-1 are equal in 0.1 M KCl, Bagshaw and Trentham suggested that this rate was a measure of k_2 or k_{-5} as these two steps have in common a transition of a bound nucleotide. The rate of the hydrolysis step (k_3) was assumed to be much greater than k_2, since the observed fluorescence transient fitted a single exponential reasonably well. The amplitude of the fluorescence change obtained when AMP-PNP binds to SF-1 was half of the change obtained with ATP. This suggested that nonhydrolyzable nucleotides bind to SF-1 in two steps, while there is a third step in the reaction with ATP in which hydrolysis occurs accompanied by an additional fluorescence increase. Measurements of fast proton release (Koretz & Taylor, 1975; Chock, 1979) also lead to similar values for the maximum rate constant and for the amount of protons released by ADP and ATP. The proton data provided additional support for the assignment of rate constants in the Bagshaw–Trentham scheme and for the release of a fraction of a proton in steps 2 and 5. This scheme provided a satisfactory synthesis of the available evidence, but recent studies have shown that a reassignment of the rate constants in the ATP binding scheme

† From the Department of Biophysics and Theoretical Biology, The University of Chicago, Chicago, Illinois 60637. *Received January 29, 1981.* This work was supported by Program Project Grant HL 20592 from the National Institutes of Health and by the Muscular Dystrophy Association of America.

[1] Abbreviations: ADP, adenosine 5′-diphosphate; AMP-PNP, adenosine 5′-(β,γ-imidotriphosphate); ATP, adenosine 5′-triphosphate; SF-1, myosin subfragment 1; ATPase, adenosinetriphosphatase; Tris, 2-amino-2-(hydroxymethyl)-1,3-propanediol; Mes, 4-morpholineethanesulfonic acid; acto-SF-1, actosubfragment 1; DEAE, diethylaminoethyl.

0006-2960/82/0421-1284$01.25/0

was necessary (Johnson & Taylor, 1978; Chock et al., 1979).

The steps in the revised scheme remain the same; however, the maximum rate observed at high ATP concentration is a measure of the hydrolysis step k_3 rather than k_2. A number of observations suggested the presence of a fast fluorescence transition, followed by a second slower transition; thus, $k_2 \gg k_3$. First, slightly biphasic fluorescence transients were observed at low temperature (3 °C), which indicated the presence of a faster transition. Second, at 20 °C there was a loss of signal amplitude from the beginning of the transient beyond that which could be accounted for by the dead time of the stopped-flow apparatus. Third, the irreversible binding of ATP occurred at a faster rate than the main fluorescence signal. The rate of the hydrolysis step was equal to the maximum observed fluorescence rate within the error of phosphate burst measurements.

In the revised scheme, which will still be referred to as the Bagshaw–Trentham mechanism, the rate constant of the slower, larger amplitude fluorescence transition for ATP (k_3) is equal to that for the ADP transition (k_{-5}) even though the processes for the two nucleotides appear to be quite different. Step 3 is considered to be the hydrolysis step for ATP while it is a transition between different bound nucleotide states for ADP.

This similarity of the rates of apparently different steps in the reactions of ADP and ATP with SF-1, which is not explained by the revised mechanism, prompted a reinvestigation of the steps in the binding of these ligands to SF-1 and acto-SF-1. The evidence presented here shows that there are two transitions that produce an enhancement of tryptophan fluorescence when ADP or AMP-PNP binds to SF-1, consistent with the mechanism

$$M_0 + L \overset{K_0}{\rightleftharpoons} M_0{\cdot}L \underset{k_{-1}}{\overset{k_1}{\rightleftharpoons}} M_1{\cdot}L \underset{k_{-2}}{\overset{k_2}{\rightleftharpoons}} M_{12}{\cdot}L \qquad (2)$$

The slower of the two rate processes observed at high nucleotide concentration is a measure of $k_2 + k_{-2}$, and $k_1 + k_{-1} \gg k_2 + k_{-2}$. The rate constant of the second fluorescence transition ($k_2 + k_{-2}$) for ADP is equal to the rate constant of the second fluorescence transition in the ATP mechanism in 0.1 M KCl, but the rates of the two processes are markedly different at higher ionic strengths.

Evidence is provided for a conformation change prior to the nucleotide-induced dissociation of actomyosin. This state could not be observed directly with ATP as the dissociating nucleotide. The kinetic scheme for the reactions of nucleotides with acto SF-1 is complex since at least three ternary complexes are necessary to account for the reactions.

Materials and Methods

Protein and Nucleotide Purification. Chymotryptic SF-1 was prepared from rabbit back and leg muscles by the method of Weeds & Taylor (1975). In a number of experiments the two SF-1 isozymes were examined separately. Actin was prepared from the acetone-dried powder by the method of Taylor & Weeds (1976). Grade 1 ADP was purchased as the sodium salt from Sigma Chemical Co. AMP-PNP was purchased as the tetralithium salt from Boehringer-Mannheim. The extinction coefficient for both nucleotides is 15.4 mM^{-1} cm^{-1} at 259 nm. It was important to ensure that there were no other nucleotide contaminants in the ADP or AMP-PNP. Before use, all nucleotides were purified on a DEAE-Sephadex A-25 column eluted with a linear gradient of 0.05–0.4 M triethylammonium bicarbonate. Purified fractions were evaporated to dryness in a rotary evaporator. This residue was redissolved in 50% methanol and evaporated repeatedly. The purified nucleotide was then dissolved in buffer and stored at −20 °C.

Kinetic Analysis. Stopped-flow measurements were made with the apparatus described by Johnson & Taylor (1978). Tryptophan fluorescence was excited at 295 nm and observed at 340 nm, employing interference filters of 10-nm bandwidths. Correction for light scattering and calibration of the fractional change in fluorescence relative to steady-state values measured with a Perkin-Elmer MPF-44A fluorometer were described by Johnson & Taylor (1978). The 90° light scattering of acto-SF-1 solutions was measured at 295 or 340 nm.

Experimental data were fitted to either a single exponential of the form $x = g_0 + g_1 \exp(-\lambda_1 t)$ or a double exponential of the form $x = g_0 + g_1 \exp(-\lambda_1 t) + g_2 \exp(-\lambda_2 t)$ by a method of moments program, which fitted the five parameters g_0, g_1, g_2, λ_1, and λ_2. Alternatively, the two phases of a biphasic transient were fitted separately to single exponentials.

Kinetic Equations. The experimental evidence on ligand binding indicated that two first-order transitions occur following the formation of a collision complex. The simplest kinetic scheme is

$$M_0 + L \overset{K_0}{\rightleftharpoons} M_0{\cdot}L \underset{k_{-1}}{\overset{k_1}{\rightleftharpoons}} M_1{\cdot}L \underset{k_{-2}}{\overset{k_2}{\rightleftharpoons}} M_{12}{\cdot}L \qquad (2)$$

$M_0{\cdot}L$ is a collision complex in which ligand L is in rapid equilibrium with free ligand (Bagshaw & Trentham, 1974). The states $M_1{\cdot}L$ and $M_{12}{\cdot}L$ are defined by different enhancements of tryptophan fluorescence. The kinetic equations for the scheme were obtained by standard methods (Benson, 1960, p 39). The concentration of a myosin–ligand state (X_i) is given by an equation of the form $X_i = g_0 + g_i \exp(-\lambda_1 t) + g_2 \exp(-\lambda_2 t)$. The constants g_i are determined from the boundary conditions, and the two rate parameters λ_i are the roots of a quadratic equation, $-\lambda_i = (1/2)[-b \pm b(1 - 4c/b^2)^{1/2}]$, where $b = \bar{k}_1 + k_{-1} + k_2 + k_{-2}$, $c = \bar{k}_1(k_2 + k_{-2}) + k_{-1}k_{-2}$, and $\bar{k}_1 = K_0 L k_1/(K_0 L + 1)$. The quantities determined experimentally are the apparent first-order rate constant for ligand binding k^a, the maximum rate constants at very high ligand concentrations, and the apparent rate constant for ligand dissociation k^d. At very low or very high ligand concentrations $4c/b^2 < 1$, and a good approximation to the λ_i is obtained by expanding the square root, $(1 - 4c/b^2)^{1/2} \approx 1 - 2c/b^2$, which gives $\lambda_2 \approx b$ and $\lambda_1 \approx c/b$. For very low ligand concentrations such that $K_0 L \ll 1$ a single exponential process was observed, and $k^a = [(d\lambda_1)/(dL)]_{L\to 0} = K_0 k_1 (k_2 + k_{-2})/(k_{-1} + k_2 + k_{-2})$. For the case $k_{-1} \ll k_2 + k_{-2}$, $k^a = K_0 k_1$. In this approximation K_1 is much greater than one. The rate of dissociation of ligand measured by blocking the reassociation step is obtained by setting $L = 0$ in λ_1; $k^d = k_{-1}k_{-2}/(k_{-1} + k_2 + k_{-2})$. The ratio k^a/k^d defines a constant that should be equal to the quantity determined in equilibrium binding studies. By direct substitution the equilibrium constant $K_{eq} = K_0(1 + K_1 + K_1K_2) \simeq K_0(K_1 + K_1K_2)$ for $K_1 \gg 1$. The kinetic constant $k^a/k^d = K_0(K_1 + K_1K_2)$.

The studies on the binding of AMP-PNP suggested that the equilibrium constant for one of the transitions was close to unity. Association could then occur by a branched pathway if the fast step has a small equilibrium constant, which increases the complexity of the kinetic equations. In the absence of evidence to the contrary it is assumed that the rate constants are independent of the order of the transitions:

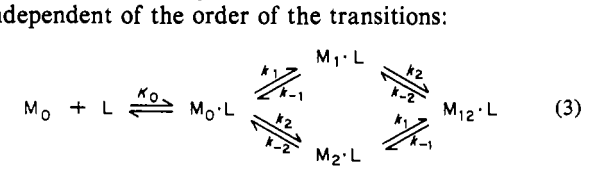

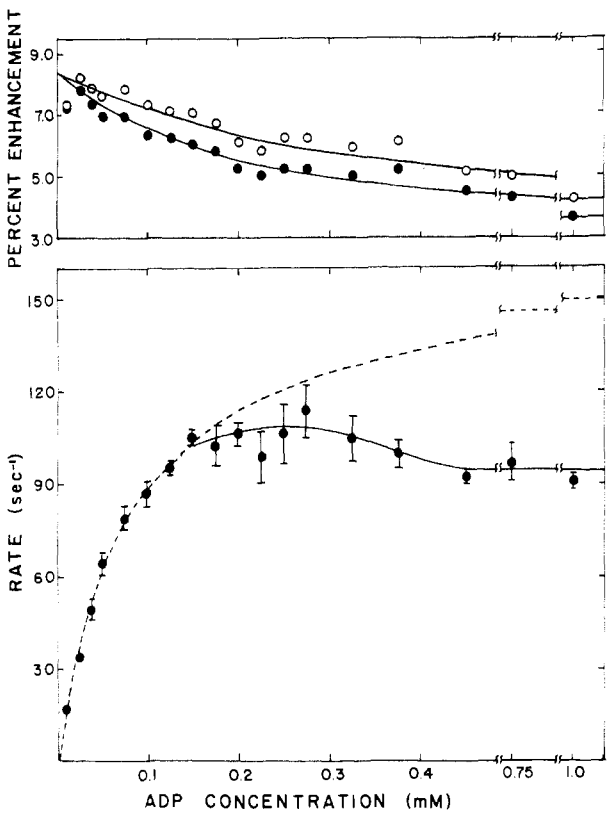

FIGURE 1: Rate and amplitude of the fluorescence enhancement of SF-1 as a function of ADP concentration. (Lower panel) The apparent rate constant λ (s^{-1}) obtained by fitting the fluorescence signal to a single exponential term, $\exp(-\lambda t)$ as a function of ADP concentration. In all figures the concentrations given are the values after mixing. The dashed curve was obtained by fitting the data for the range of concentrations up to 150 μM ADP to a hyperbola. The solid line was drawn through the data points for concentrations larger than 150 μM. Error bars indicate the standard deviation of 3–4 experimental traces. (Upper panel) The percent fluorescence enhancement of the observed transient signal relative to SF-1 (●). The open circles (○) refer to the enhancement corrected for loss of signal in the dead time of the apparatus according to the equation $A_{corr} = A_{obsd} \exp(\lambda T)$ where λ is the observed rate and T is the dead time (1.5 ms). Experimental conditions: 10 mM Tris–Mes, pH 7, 0.1 M KCl, 5 mM $MgCl_2$, 3 μM SF-1, 20 °C.

For the case that K_1 is small, $k_1 + k_{-1}$ is much larger than $k_2 + k_{-2}$, and k_{-2} is very small. It is assumed that $M_2{\cdot}L$ and $M_{12}{\cdot}L$ are essentially in equilibrium and that k_{-2} can be neglected. In this case the solution of the rate equations has the same form as before with $b = \bar{k}_1 + \bar{k}_2 + k_{-1} + k_2$, $c = (\bar{k}_1 + \bar{k}_2)k_2 + \bar{k}_2 k_{-1}$, and $\bar{k}_2 = K_0 L k_2/(K_0 L + 1)$. In the limit of low ligand concentrations $k^a = K_0 k_2(k_1 + k_{-1} + k_2)/(k_{-1} + k_2) \simeq K_0(K_1 + 1)k_2$ for $k_{-1} \gg k_2$. Applications of kinetic equations to the reactions of ligands with actomyosin were based on extensions of the same methods.

Results

ADP Binding to SF-1. The kinetics of binding of ADP to SF-1 and the amplitudes of the fluorescence enhancement were first examined at 20 °C in 0.1 M KCl for comparison with evidence reported previously by Bagshaw and Trentham. The time course of the fluorescence transient was fitted reasonably well by a single exponential term in agreement with their findings. The variation in the apparent rate constant as a function of ADP concentration is shown in Figure 1 (lower panel). The rate constant increased to a maximum value and then decreased slightly at higher nucleotide concentration. The dashed line in Figure 1 shows the fit of a hyperbola to the data for concentrations less than 150 μM ADP. At higher ADP concentrations the observed rate clearly deviates from the hyperbolic fit. This behavior is very similar to that reported for ATP binding to SF-1 (Johnson & Taylor, 1978). The apparent second-order rate constant under these conditions (20 °C, 0.1 M KCl, pH 7) is 1.6×10^6 M^{-1} s^{-1}, and the maximum rate is 95 ± 10 s^{-1}.

The corresponding amplitudes of the observed fluorescence transients are also shown in Figure 1 (upper panel). The percent fluorescence enhancement is the change in fluorescence upon binding of nucleotide relative to the fluorescence of SF-1 ($\Delta F/F_{SF\text{-}1}$). In this experiment, the observed amplitude of the transient (filled circles) decreased from 8% enhancement at low ADP concentrations to 4% at high ADP concentration. The amplitude continued to decrease even after the maximum rate had been attained. The open circles show the percent fluorescence enhancement corrected for the apparatus dead time of 1.5 ms with the observed rate constant (see Figure 1 legend). It should be emphasized that the loss in observed signal amplitude arises from signal missing from the beginning of the transient at zero time. The final voltage remained the same at all ADP concentrations. The signal loss was not caused by absorption of the incident beam, since the transmitted beam voltage remained constant over the entire range of ADP concentration.

These two observations, nonhyperbolic dependence of rate on ADP concentration and loss of signal amplitude, suggest the presence of a faster fluorescence transition, which is not resolved from the signal of a second slower transition. The signal loss can be accounted for by a fast phase at the beginning of the transient, which becomes fast enough to be completed during the dead time of the instrument. From the total amplitude of the signal at low ADP concentration and the amount of signal that remains at high nucleotide concentration, each of the two fluorescence transitions result in a 4–5% fluorescence enhancement. Because the two fluorescence transitions are not well separated at 20 °C, the observed rate constant at intermediate ADP concentration obtained by fitting to a single exponential term is a mixture of the fast and slow rate constants. This leads to a maximum observed rate at intermediate ADP concentration, followed by a slight decrease at higher nucleotide concentration to the value of the rate constant of the second transition. This type of behavior was analyzed previously by Johnson & Taylor (1978) for the reaction of SF-1 with ATP.

More direct evidence for two fluorescence transitions was obtained at lower temperatures. When ADP was mixed with SF-1 in the stopped-flow apparatus at either 2 or 10 °C, markedly biphasic transients were obtained. An experimental transient at 3 °C is shown in Figure 2A. The second slower fluorescence transition was fitted to a single exponential following the fast phase, as indicated by the smooth line through the jagged trace. The maximum rate of this second slower transition is 15 ± 2 s^{-1} at 3 °C, 34 ± 6 s^{-1} at 10 °C, and 95 ± 10 s^{-1} at 20 °C. The maximum rate of the fast transition was estimated to be 180 s^{-1} at 3 °C and 300 s^{-1} at 10 °C. At 20 °C the rate of the fast fluorescence signal would be on the order of 1000 s^{-1}, based on the temperature dependence, and thus 95% of the signal from this transition would be lost in 2 ms. The amplitudes of the two fluorescence transitions at lower temperature were approximately 5% each, which agreed with the value obtained from the signal loss at 20 °C. The biphasic fluorescence transients cannot be explained by two classes of SF-1 with different binding constants for ADP, since experiments that used SF-1 with only the A1 light chain gave identical results with experiments done with a mixture of SF-1 A1 and SF-1 A2.

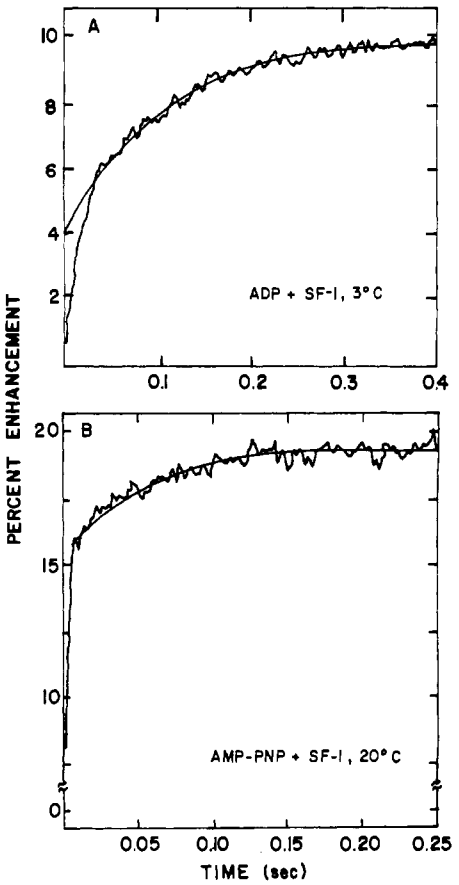

FIGURE 2: Biphasic fluorescence signals for the reaction of SF-1 with ADP and AMP-PNP. The jagged curve represents the actual data of the time dependence of the fluorescence increase, while the smooth curve is the computer-generated fit to the data. The percent fluorescence enhancement was calculated relative to SF-1. (A) Biphasic fluorescence transient following the mixing of ADP and SF-1 at 3 °C. The rate of the slow fluorescence transition is 10 s^{-1}. Experimental conditions: 10 mM Tris–Mes, pH 7, 0.1 M KCl, 5 mM $MgCl_2$, 3 μM SF-1, and 50 μM ADP, 3 °C. (B) Biphasic fluorescence transient obtained after mixing AMP-PNP with SF-1 at 20 °C. The rate constants are 250–300 s^{-1} for the fast transition and 15–20 s^{-1} for the slow transition. Experimental conditions: 10 mM Tris–Mes, pH 7, 0.1 M KCl, 5 mM $MgCl_2$, 3 μM SF-1, and 3 mM AMP-PNP, 20 °C.

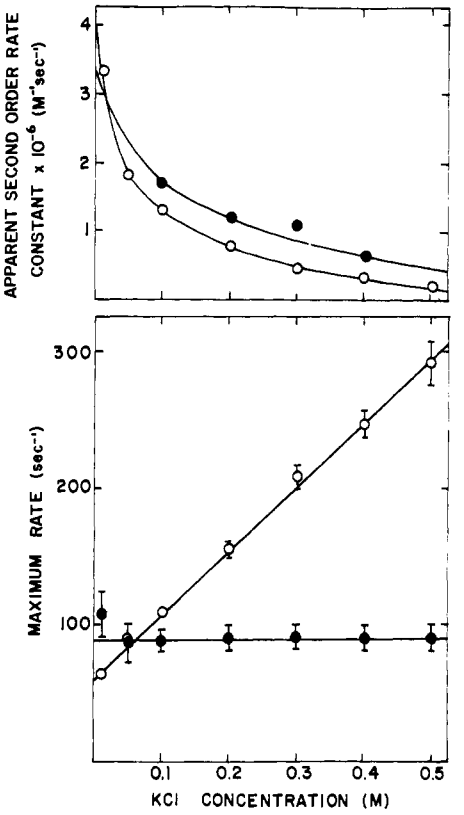

FIGURE 3: Ionic strength dependence of the apparent second-order rate constant and the rate constant ($k_2 + k_{-2}$) for the reactions of ADP and ATP with SF-1. The data were fitted to a single exponential term. In the lower panel, the maximum rate of the fluorescence transient was determined at a final nucleotide concentration of 1 mM. The filled circles (●) show the maximum rate obtained for ADP, and the open circles (○) show the maximum rate obtained for ATP. In the upper panel, the apparent second-order rate constant K_0k_1 (M^{-1} s^{-1}) was obtained from the initial slope of the plot of rate vs. nucleotide concentration. The filled circles (●) represent ADP and the open circles (○) ATP. The curve fitted to the data was calculated from the Debye–Hückel limiting law. Experimental conditions: 10 mM Tris–Mes, pH 7, 5 mM $MgCl_2$, and 3 μM SF-1, 20 °C.

The rate constant of the slower transition obtained with ADP (20 °C, 0.1 M KCl, pH 7) is the same as the rate constant observed with ATP. However, this equality did not hold under all conditions. The ionic strength dependence of the rate constants of the ADP and ATP reactions are shown in Figure 3 (bottom). The maximum rate of the ADP fluorescence signal (filled circles) is essentially independent of ionic strength, while the rate for ATP (open circles) increased markedly with ionic strength as previously reported (Johnson & Taylor, 1978). The curves cross in the vicinity of 0.1 M KCl. Thus the similarity in rate constants for the two reactions, which had been noted previously (Bagshaw et al., 1974), is seen to be fortuitous.

The upper graph (Figure 3) shows the apparent second-order rate constant as a function of ionic strength for the two nucleotides. The apparent second-order rate constant ($k^a \simeq K_0k_1$ for the three-step model) is the initial slope of the rate vs. nucleotide concentration plot. The rate constant decreased with increasing ionic strength in a similar manner for both ADP and ATP. The curves drawn through the data fit the Debye–Hückel limiting law with a charge product of −1.2 for $MgADP^{-1}$ as compared with the previously reported value of −1.9 for $MgATP^{-2}$ (Johnson & Taylor, 1978).

The amplitude of the fluorescence change when ADP binds to SF-1 increased with ionic strength from 10 ± 2% at 0.1 M KCl to 13.5 ± 2% at 0.6 M KCl (Table I). The error limits refer to averages from several experiments. For any particular preparation the amplitude of the fluorescence change consistently increased with ionic strength. The variation does not seem to be an effect on the equilibrium constant of the second fluorescence transition. No fluorescence signal was observed in the stopped-flow apparatus at the rate of the second transition when SF-1·ADP was mixed with various concentrations of KCl, even though the final level of fluorescence increased with KCl concentration. There was no change in fluorescence when SF-1 alone was mixed with the same concentrations of KCl.

AMP-PNP Binding to SF-1. The kinetics of binding of the nonhydrolyzable nucleotide AMP-PNP to SF-1 and the amplitude of the fluorescence enhancement were also reinvestigated. When AMP-PNP was mixed with SF-1, two fluorescence transitions were resolved at 20 °C (0.1 M KCl, pH 7), as shown by the experimental transient obtained at 3 mM AMP-PNP (Figure 2B).

The variation of the rate of the reaction with ligand concentration is illustrated in Figure 4. At very low concentrations, in the range from 5 to 75 μM the rate process adequately fitted a single exponential term. The plot is linear and the slope gives k^a, which is (1–2) × 10^5 M^{-1} (open squares in

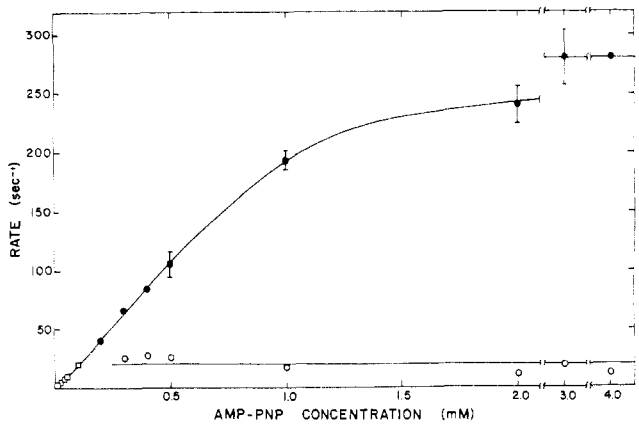

FIGURE 4: Dependence of the two rate processes on nucleotide concentration for the reaction of SF-1 with AMP-PNP. For AMP-PNP concentrations <0.1 mM, the fluorescence transient was adequately fitted by a single exponential (open squares) and the apparent rate constant increased linearly with concentration and corresponded to an apparent second-order rate constant of (1–2) × 10^5 M^{-1} s^{-1}. As the nucleotide concentration was increased, a faster process of small amplitude was observed. At concentrations >0.25 mM the amplitude of the fast transition was larger, and the two apparent rate constants λ_1 and λ_2 were easily separated as shown by the open and filled circles. Error bars indicate the standard deviation of 3–4 experimental transients. Experimental conditions: 10 mM Tris–Mes, pH 7, 0.1 M KCl, 5 mM $MgCl_2$, 3 μM SF-1, 20 °C.

Figure 4). As the nucleotide concentration was increased further, a faster process of small amplitude was observed, but an accurate fit to two exponential terms could not be made until the amplitude was approximately 25% of the total. At still higher concentrations the two apparent rate constants λ_1 and λ_2 are easily separated (open and filled circles). At very high AMP-PNP concentration the fast step (λ_2) contributed 75% of the signal. The maximum rates were λ_2 approximately 250–300 s^{-1} and λ_1 approximately 20 s^{-1}. It should be emphasized that λ_1 and λ_2 are not in general the rate constants as described under Kinetic Equations. However, the maximum values are approximately $k_1 + k_{-1}$ for the fast process and $k_2 + k_{-2}$ for the slow process. The shape of the plot of the faster process vs. concentration is not a hyperbola, but the half-maximum value provides a rough estimate of the equilibrium constant of the initial binding step [$K_0 \simeq (1–2) \times 10^3$ M^{-1}].

The same fit to two exponential terms was obtained with the SF-1 (A-1) isozyme; thus, the two processes occur for a single type of SF-1. However, the evidence does not require that the two first-order transitions occur in sequence except that the large ratio of the two rate constants could determine a dominant pathway in which the faster transition occurs first.

The kinetic data are summarized in Table II. The rate constants $k_1 + k_{-1}$ and $k_2 + k_{-2}$ are 4–5 times smaller for AMP-PNP compared to ADP or ATP, and the apparent second-order rate constant is 10 times smaller. The amplitudes of the two transitions of SF-1·AMP-PNP in 0.1 M KCl are 11 ± 3% for the fast step and 4 ± 2% for the slow step. In 0.6 M KCl, the total amplitude increased to 24 ± 3% and consisted typically of 18% for the fast step and 6% for the slow step. At the higher ionic strength the apparent second-order rate constant decreased 5-fold; consequently, the ionic strength dependence of the maximum rate of the fast isomerization could not be determined since the rate was still linear in AMP-PNP concentration at 1 mM. The observed rate constant for the slower transition was essentially independent of ionic strength, as also observed for ADP.

Dissociation of Acto-SF-1 by AMP-PNP and ADP. AMP-PNP is more effective in dissociating acto-SF-1 than

Table I: Rate Constants for ADP Binding to SF-1 and Acto-SF-1[a]

protein	conditions	app second-order rate constants k^a [(M^{-1} s^{-1}) × 10^{-4}]	fast fluorescence transition (s^{-1})	slow fluorescence transition (s^{-1})	dissociation of acto-SF-1 (s^{-1})	dissociation of nucleotide (s^{-1})	percent fluorescence enhancement
SF-1	0.1 M KCl, 20 °C	170 ± 20	1000–1500	90 ± 10		1.4	10 ± 2
	0.1 M KCl, 4 °C	35 ± 10	170 ± 20	15 ± 5		0.07	10 ± 2
	0.6 M KCl, 20 °C	50 ± 10		90 ± 10			13 ± 2
acto-SF-1	0.1 M KCl, 20 °C				1.0 ± 0.2 (L.S.)	>500	0
	0.6 M KCl, 20 °C				0.6 ± 0.1 (L.S.)		0

[a] Rate constants were determined from transients obtained following mixing of nucleotide with SF-1 or acto-SF-1 in the stopped-flow apparatus. The rate constants were obtained from fluorescence transients or from light scattering transients (L.S.) in the case of acto-SF-1. The observed rates are functions of the individual rate constants as described for various schemes under Kinetic Equations. For ADP binding to SF-1, the rates obtained refer to mechanism 2 where the apparent second-order rate constant k^a is approximately K_0k_1, the fast fluorescence transition is $k_1 + k_{-1}$, and the slow fluorescence transition is $k_2 + k_{-2}$. The percent fluorescence enhancement was obtained from equilibrium measurements in the fluorescence spectrophotometer and is the change in fluorescence relative to that obtained with chymotryptic SF-1 ($\Delta F/F_{SF\text{-}1}$). Error limits refer to average values obtained from different preparations. Experimental conditions: 10 mM Tris–Mes, pH 7, 5 mM $MgCl_2$, and other conditions as noted. Dissociation of ADP from SF-1 at 4 °C was measured by displacement with pyrophosphate (Sleep et al., 1981).

ADP both in the extent and rate of dissociation. In 0.1 M KCl (20 °C, pH 7) ADP produced only 55% dissociation of 3 μM acto-SF-1 as measured by light scattering, while AMP-PNP gave 85% dissociation. ATP yielded at least 90% dissociation under the same conditions. The rate of dissociation by ADP reached a maximum value of approximately 1 s^{-1}, but the rate for AMP-PNP was faster and continued to increase linearly with concentration. At 4 mM AMP-PNP the rate of dissociation was 40 s^{-1}, which gives an apparent second-order rate constant for binding of 10^4 M^{-1} s^{-1}.

The extent of dissociation increased with increasing ionic strength, but the apparent second-order rate constant for AMP-PNP binding and the maximum rate of dissociation by ADP decreased with ionic strength. A maximum rate of dissociation by AMP-PNP was not reached at any ionic strength although at very low ionic strength (5 mM KCl) the rate vs. concentration plot was no longer linear, and a rough estimate of the maximum rate is 100–200 s^{-1}. The data at high and low ionic strength are summarized in Tables I and II.

The fluorescence change associated with the nucleotide-induced dissociation of acto-SF-1 was investigated. Tables I and II show the amplitude of the fluorescence change at equilibrium when acto-SF-1 was dissociated by ADP or AMP-PNP at two different ionic strengths. It was shown previously that dissociation of acto-SF-1 results in a 10–14% decrease in fluorescence (Johnson & Taylor, 1978). The amplitude of the fluorescence increase when ADP binds to SF-1 at 0.1 M KCl or 0.6 M KCl or when AMP-PNP binds to SF-1 at 0.1 M KCl is approximately the same magnitude as the decrease in fluorescence that accompanies acto-SF-1 dissociation. Thus, no net fluorescence change should be observable under these conditions. However, the amplitude of fluorescence signal increases with ionic strength for AMP-PNP binding to SF-1 to a value of 24 ± 2% in 0.6 M KCl. Dissociation of acto-SF-1 gave a fluorescence enhancement of 14 ± 2% at this ionic strength, which agrees with the net signal expected from the combination of the binding and dissociation steps (Table II).

The time course of this fluorescence increase and of the light scattering decrease when 0.4 mM AMP-PNP (final concentration) was mixed with acto-SF-1 at 0.6 M KCl is shown in Figure 5B. A rapid fluorescence increase with a rate of 15 s^{-1} was followed by a slower transition with a rate of approximately 1.5 s^{-1}. The rate of dissociation as observed from the decrease in light scattering (dashed line) was 1.3^{-1}, and thus the rate was essentially the same as the slower fluorescence step of the biphasic transient. The first fluorescence transition occurred at a rate that was faster than the light scattering signal, that is, prior to dissociation. Under the same conditions, when SF-1 was reacted with AMP-PNP, the fluorescence transient (Figure 5A) was also biphasic with a fast phase of 13 s^{-1} and a slower phase of 9 s^{-1}. Thus the rate of the fast fluorescence transition was approximately the same for the binding of AMP-PNP to SF-1 or acto-SF-1, while the apparent second-order binding constant determined from light scattering was approximately 10 times less.

Figure 6 shows the rate of the slower fluorescence transition for the binding of AMP-PNP to SF-1 (filled circles) or acto-SF-1 (open circles) and the rate of the light scattering signal (open triangles) measured as a function of AMP-PNP concentration. The rate constant of the slower fluorescence transition agreed with the rate constant of dissociation measured by light scattering over a range of nucleotide concentrations and was approximately 10-fold slower than the corresponding fluorescence transition for SF-1. The amplitudes of the fluorescence enhancement of acto-SF-1 expressed relative to SF-1 were approximately 9% for the fast transition and 5% for the slow transition, compared with 18% and 6%

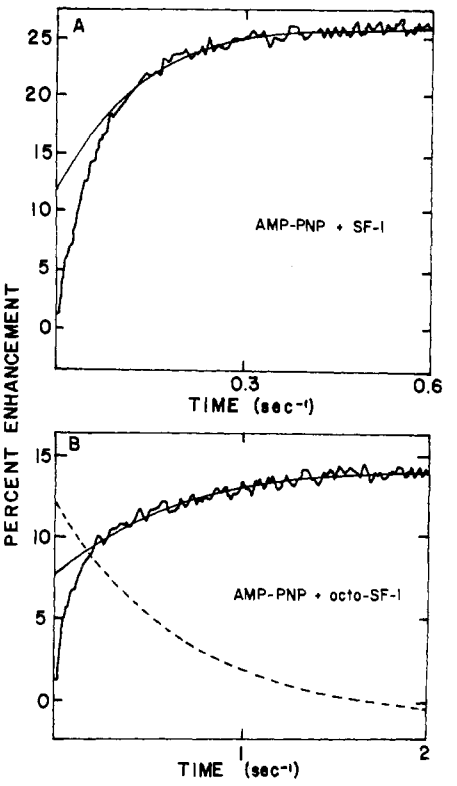

FIGURE 5: Time course of the fluorescence enhancement and light scattering signals for the reaction of AMP-PNP with SF-1 and acto-SF-1. The jagged curve represents the experimental trace, and the smooth curve represents the computer-generated fit to a single exponential for the slower fluorescence signal. The dashed line indicates the light scattering transient. (A) Fluorescence transient obtained when AMP-PNP (0.4 mM final concentration) was mixed with SF-1. The rate constant for the slower transition is 8.3 s^{-1}. (B) Fluorescence transient and the light scattering signal when the same concentration of AMP-PNP was mixed with acto-SF-1. The light scattering transient had a rate of 1.3 s^{-1} and the slower fluorescence transition a rate of 1.6 s^{-1}. The percent fluorescence enhancement is calculated relative to SF-1. Final concentrations: 3 μM SF-1 or acto-SF-1 and 400 μM AMP-PNP. Experimental conditions: 10 mM Tris–Mes, pH 7, 0.6 M KCl, 5 mM $MgCl_2$, 20 °C.

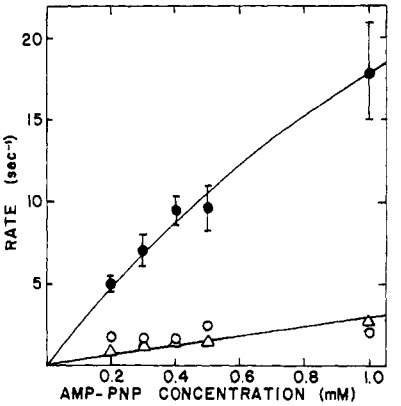

FIGURE 6: Rate parameter of the slow fluorescence transition and light scattering transient as a function of AMP-PNP concentration for SF-1 and acto-SF-1. The apparent rate constant of the slower fluorescence transition for the binding of AMP-PNP to SF-1 (filled circles) is compared with the apparent rate constant of the slower fluorescence transition (open circles) and the apparent rate constant of dissociation measured by light scattering (open triangles) for the reaction of AMP-PNP with acto-SF-1.

Table II: Rate Constants for AMP-PNP Binding to SF-1 and Acto-SF-1[a]

protein	conditions	app second-order rate constants k^a [$(M^{-1} s^{-1}) \times 10^{-4}$]	fast fluorescence transition (s^{-1})	slow fluorescence transition (s^{-1})	dissociation of acto-SF-1 (s^{-1})	dissociation of nucleotide k^d (s^{-1})	percent fluorescence enhancement
SF-1	0.1 M KCl, 20 °C	20 ± 10	300 ± 50	20 ± 5		0.02	15 ± 3
	0.1 M KCl, 4 °C	2 ± 1	>30	>4		<0.01	
	0.6 M KCl, 20 °C	4 ± 1	>60	>20			24 ± 3
acto-SF-1	0.1 M KCl, 20 °C	1.1 ± 0.1 (L.S.)			>50 (L.S.)	>500 (20 mM KCl)	0
	0.6 M KCl, 20 °C	0.2 ± 0.1 (L.S.)	>30	>3	>3 (L.S.)		14 ± 2
		2 ± 1 (fluorescence)					

[a] See Table I legend for experimental conditions. The fast and slow fluorescence transitions of SF-1 refer to rate constants $k_1 + k_{-1}$ and $k_2 + k_{-2}$, respectively. The interpretation of K^d for a sequential or branched pathway is discussed in the text.

for the reaction of AMP-PNP with SF-1 alone under these conditions.

The evidence indicates a sequential process in which the bound nucleotide first induces a change in conformation of acto-SF-1 prior to dissociation. The corresponding process has not been observed previously with ATP because of cancellation of the fluorescence signals and the very fast dissociation of the actomyosin–ATP intermediate state. A small fluorescence signal prior to dissociation was also observed with ADP at a very high ionic strength (0.8 M KCl).

Rate of Nucleotide Dissociation from SF-1 and Acto-SF-1. The rate of dissociation of AMP-PNP and ADP from SF-1 was measured by Bagshaw et al. (1972) and Bagshaw & Trentham (1974) respectively, by reacting the complex with ATP. The increase in fluorescence as ADP or AMP-PNP is replaced by ATP provides a signal that monitors the rate of spontaneous dissociation. The same method was used in the present studies. The signal fitted a single exponential term and yielded values of 1.4 s^{-1} for ADP and 0.02 s^{-1} for AMP-PNP (0.1 M KCl, 20 °C, pH 7) in reasonable agreement with the published values. The apparent rate constant for the dissociation of ADP from the acto-SF-1·ADP complex was investigated by White (1977) by measuring the rate of dissociation of the two proteins by ATP. It was expected that at a sufficiently high ATP concentration the rate of dissociation would reach a maximum determined by the rate constant of ADP dissociation. However, no maximum rate was found and White assigned a minimum rate constant of 400 s^{-1} for ADP dissociation at 4 °C. Similar results were obtained in this study. For ADP in 20 mM or 0.1 M KCl at 20 °C the rate constant of ADP dissociation was greater than 500 s^{-1}. In the case of AMP-PNP the acto-SF-1 complex was largely dissociated in 0.1 M KCl, but in 20 mM KCl dissociation was 20% or less. Reaction with ATP again produced dissociation at a rate that increased linearly with ATP concentration, and the rate constant for dissociation of AMP-PNP must be larger than 500 s^{-1}.

Although it can be concluded that both nucleotides dissociate very rapidly from acto-SF-1, the results are difficult to explain by any simple mechanism. The ratio of the apparent rate constants of association and dissociation of AMP-PNP from acto-SF-1 gives an association constant of $10–10^2$ M^{-1} (Table II), which is much smaller than the value of $(1–5) \times 10^3$ M^{-1} obtained by equilibrium measurements (Hofmann & Goody, 1978; Greene & Eisenberg, 1978). A possible explanation of the results is that the acto-SF-1–ligand complex is a mixture of states and the very fast dissociation of ligand refers to the rate of dissociation from the predominant state. The existence of at least two and possibly three ternary complexes can be inferred from the studies of dissociation described in the last section.

Further information on ternary complexes was obtained by examining the association of SF-1–ligand with actin at low ionic strength and high concentrations of SF-1–ligand. The association constant of nucleotide with SF-1 is much larger than with acto-SF-1. Consequently at a ligand concentration of 10^{-4} M, SF-1 is saturated with ligand but the ligand is nearly completely released upon reaction with actin. The rate of dissociation by ATP is now determined by the rate at which the system proceeds through the various ternary intermediates prior to the release of ligand.

The association of SF-1·ADP with actin in the absence or presence of 0.5 mM MgATP is shown in Figure 7A (30 μM SF-1·ADP, 0.25 mM free ADP, 5 μM actin, and 5 mM KCl, 20 °C). The reaction was 60% complete in the dead time of

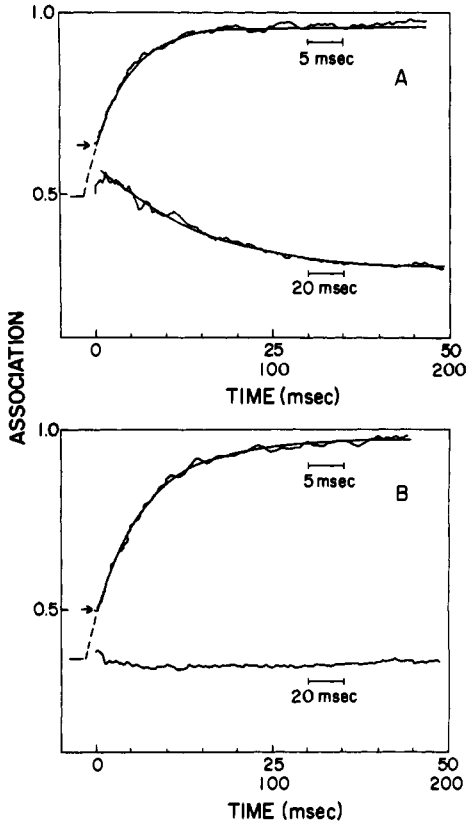

FIGURE 7: Association of SF-1–ligand complex with actin. (A) Reaction of SF-1·ADP with actin measured by light scattering; 30 μM SF-1·ADP and 0.25 mM ADP reacted with 5 μM actin (upper curve) or 5 μM actin and 0.5 mM ATP (lower curve). Concentrations refer to values after mixing; experimental conditions are 5 mM KCl, pH 7.0, 20 °C. The dashed extension of the upper curve to −1.5 ms gives the initial voltage level of the observed reaction corrected for apparatus dead time. The initial degree of reaction of almost 0.5 corresponds to a rapid equilibrium binding step, which is completed in the mixing and dead time of the apparatus. The time scale for the lower curve is 4 times larger than for the upper curve. (B) Reaction of SF-1·AMP-PNP with actin. Same conditions as (A) except ADP was replaced by 0.2 mM AMP-PNP in the SF-1 solution.

the apparatus (1.4 ms). After flow stopped a signal was observed at a rate of 150–200 s^{-1}. The signal voltage was constant for at least the final third of the drive time, which permitted the extent of the very fast reaction to be measured. The dead time of the stopped-flow apparatus is 1.4 ms. Extrapolation of the fitted curve of the observed rate process to −1.4 ms, as shown by the dashed curve in Figure 7A, gave the amplitude of the signal generated in the very fast reaction. In the example shown the amplitude was 45% of the signal for complete association. Since the initial reaction was complete in 1.5 ms, the effective rate must be much greater than 1000 s^{-1}. Thus the initial reaction is a rapid equilibrium binding of SF-1·ADP to actin. From the variation of the amplitude of the initial reaction with SF-1·ADP concentrations an equilibrium constant of 3×10^4 M^{-1} was estimated.

The rate constant of the observed signal increased from about 75 s^{-1} to 175 ± 25 s^{-1} over the range of SF-1·ADP concentrations from 10 to 30 μM. From these data and the degree of initial association a rough estimate for the rate constant of the second step is 350–400 s^{-1}.

In the presence of ATP the initial very fast association still occurred but there was only a small further increase in association, and the system dissociated to the levels obtained in the absence of ADP (i.e., the degree of association for the steady-state hydrolysis of ATP by acto-SF-1). The rate constant of the dissociation phase decreased with increasing ADP concentrations in the range from 0.1 to 1 mM. This variation arises from the competition of ADP and ATP for the nucleotide binding site. The rate constant also decreased as the ratio of SF-1·ADP to actin was increased, which indicates that this process is determined by the time for the excess S1·ADP to cycle through the association and ADP release steps.

The behavior is accounted for by at least a three-step mechanism:

$$M{\cdot}L + A \overset{K_0}{\rightleftharpoons} (A{\cdot}M{\cdot}L)_1 \overset{k_1}{\rightleftharpoons} (A{\cdot}M{\cdot}L)_2 \overset{\text{fast}}{\rightharpoonup} A{\cdot}M + L$$

The first step is the formation of a collision complex in rapid equilibrium with free M·L. This step is followed by a transition to a state in which actin is more strongly bound and ligand is more weakly bound. The rate of dissociation of ligand from state 2 is faster than k_1 (300–400 s^{-1}) because the presence of ATP prevents state 2 from accumulating. The initial association constant K_0 is 2–3 times larger than the average association of SF-1 intermediates of the steady-state cycle, and in the presence of ATP the degree of dissociation increases as SF-1·ADP is converted to the ATPase cycle intermediates. The experiment suggests that the effective rate of dissociation of ADP is determined by k_1. However, at equilibrium state 2 or other intermediates to which actin is strongly bound are the major species present, and the very fast rate of dissociation measured for an equilibrium mixture refers to dissociation from these intermediates.

An example of a similar experiment with AMP-PNP as ligand is shown in Figure 7B. In this case the initial association is smaller but the rate constant of the second step is approximately the same as for ADP. The second step in the association process was not observed in the presence of ATP, but the decrease in association was very small because the initial association of SF-1·AMP-PNP with actin was nearly equal to the degree of association in the steady-state ATPase cycle.

Discussion

The mechanism of the reaction of the nonhydrolyzable nucleotides ADP and AMP-PNP with SF-1 is more complex than was recognized in previous studies. Two first-order transitions were detected by the enhancement of tryptophan fluorescence, which are easily resolved for AMP-PNP at 20 °C and for ADP at lower temperatures. The two transitions are not explained by differences between two isozymes since both transitions also occur for SF-1 (A1). At low ligand concentrations only a single rate process is observed, which is consistent with a two-step sequential mechanism rather than two independent molecules with different properties. In the case of ATP, which binds to the same site, the two fluorescence transitions are known to occur in sequence since ATP, which is tightly bound in the fast step, is hydrolyzed at a rate corresponding to the slower step (Johnson & Taylor, 1978). Independent evidence for two strongly bound SF-1–nucleotide states that are in equilibrium has been presented by Shriver & Sykes (1981), based on ^{31}P NMR measurements. They observed two intermediates for the same condition in which two fluorescence transitions were easily resolved in this study, namely, AMP-PNP at 20 but not at 3 °C and ADP at 3 but not at 20 °C.

Because the apparent second-order rate constant for ligand association was relatively small, particularly for AMP-PNP, it is probably not the actual rate constant for the first step, and the association is not explained by a simple ligand binding reaction (Gutfreund, 1975). The most probably alternative (Bagshaw & Trentham, 1974) is the formation of a weakly

bound collision complex that is in equilibrium with free ligand, followed by two first-order transitions that produce more tightly bound nucleotide states. The evidence does not require a preferred order for the two transitions; however, the 5–10-fold ratio of the rate constants could lead to a dominant pathway. Therefore, the following branched mechanism has to be considered initially:

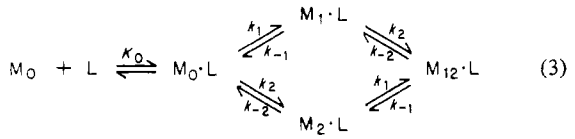

(3)

States 1, 2, and 12 have enhanced tryptophan fluorescence, but the notation introduced by Bagshaw and Trentham in which asterisks are used to denote relative fluorescence intensity is not suitable. Since we do not have evidence to the contrary, it will be assumed that the transitions are independent; that is, the rate constants of the step $M_0{\cdot}L \rightleftharpoons M_1{\cdot}L$ are the same as the step $M_2{\cdot}L \rightleftharpoons M_{12}{\cdot}L$. Solution of the kinetic equations shows that the observed rate constants of the fast and slow rate processes are approximately equal to $k_1 + k_{-1}$ and $k_2 + k_{-2}$, respectively. However, it is necessary to distinguish two cases. If K_1 is large, the association reaction will follow essentially a single pathway because $k_1 + k_{-1} \gg k_2 + k_{-2}$ and $k^a = K_0k_1$. If K_1 is close to unity, both pathways make approximately equal contributions and $k^a = K_0(K_1 + 1)k_2$.

The reaction of SF-1 with ADP at 20 °C is explained by predominantly a single pathway. The first-order transitions have the same rates in 0.1 M KCl as the corresponding steps of the ATP reaction

$$M_0 + ATP \overset{K_0}{\rightleftharpoons} M_0{\cdot}ATP \underset{k_{-1}}{\overset{k_1}{\rightleftharpoons}} M_1{*}{\cdot}ATP \underset{k_{-2}}{\overset{k_2}{\rightleftharpoons}} M_{12}{**}{\cdot}ADP{\cdot}P_i$$

although $k_2 + k_{-2}$ increases with ionic strength for ATP but not for ADP (Figure 3). The apparent second-order rate constant also has a different dependence on ionic strength, but the difference is explained by the electrostatic interaction of $MgATP^{2-}$ vs. $MgADP^{1-}$ with a positive charge at the binding site.

The apparent rate constant of dissociation of ADP and AMP-PNP from SF-1 has been measured by displacement with other ligands (Bagshaw & Trentham, 1974; Bagshaw et al., 1972; Sleep et al., 1981, and present work). In the case of a single pathway (mechanism 2), $k^d = k_{-1}k_2/(k_{-1} + k_2 + k_{-2})$ and since K_1 is large, a single rate process would be observed. The kinetic measurements are not sufficient to unambiguously determine k_{-1} and k_{-2}, but limits can be placed on the range of values. For ADP at 20 °C the rate of dissociation requires that k_{-1} and k_{-2} cannot both be the same magnitude as k^d (1.4 s^{-1}); hence, both equilibrium constants must be fairly large, which is consistent with the presence of a single β-phosphate peak in the NMR spectrum.

Values for K_1 of 40–100 and K_2 of 10–20 are consistent with the measured values of k^d, k^a, $k_1 + k_{-1}$, and $k_2 + k_{-2}$. A resonable fit is

$$M_0 + L \overset{K_0 = 10^3}{\leftrightarrow} M_0L \underset{20}{\overset{1000}{\rightleftharpoons}} M_1L \underset{10}{\overset{100}{\rightleftharpoons}} M_{12}L$$

K_0 is the equilibrium constant (M^{-1}) for the initial rapid equilibrium step, and the remaining numbers in units of s^{-1} are the rate constants k_1/k_{-1} and k_2/k_{-2}, respectively. At 3 °C, $k^d = 0.07$ s^{-1} and one equilibrium constant is 2.0 or 0.5, depending on the assignment of the states (Shriver & Sykes, 1981). The best fit was obtained for

$$M_0 + L \overset{K_0 = 10^3}{\leftrightarrow} M_0L \underset{0.2}{\overset{180}{\rightleftharpoons}} M_1L \underset{5}{\overset{10}{\rightleftharpoons}} M_{12}L$$

The occurrence of two conformation changes in nucleotide binding, irrespective of hydrolysis, may explain the fast release of 0.2–0.3 mol of hydrogen ion both by the nonhydrolyzable nucleotides and by ATP (Bagshaw & Trentham, 1974; Koretz & Taylor, 1975; Marsh et al., 1977; Chock, 1979). It was concluded previously that the proton did not come from the hydrolysis step because hydrolysis is not required for proton release, yet the rate is approximately the same for ADP and ATP and is equal to $k_2 + k_{-2}$. Furthermore, step 2 had the same pH dependence of the rate and amplitude of the H^+ burst for ADP and ATP (Sleep et al., 1981). The amplitude of the phosphate burst also decreased slightly with decreasing pH, which is consistent with proton release in hydrolysis (Taylor, 1977). Rather than postulating a different mechanism for ADP binding (Chock, 1979), we conclude that two conformation changes occur in nucleotide binding independently of whether hydrolysis occurs, and the slower transition involves the same change in environment of one or more ionizable residues.

In the case of AMP-PNP at 20 °C the very small rate of nucleotide dissociation ($k^d = 0.2$ s^{-1}) can only be accounted for by making one of the reverse rate constants approximately equal to k^d. Consequently one of the equilibrium constants is large and the other is close to unity in agreement with the results of Shriver & Sykes (1981). The kinetic data could be explained by taking a large equilibrium constant for the fast step (K_1) that gives an essentially sequential pathway:

$$M_0 + L \overset{K_0 = 10^3}{\rightleftharpoons} M_0{\cdot}L \underset{0.05}{\overset{250}{\rightleftharpoons}} M_1{\cdot}L \underset{10}{\overset{10}{\rightleftharpoons}} M_{12}{\cdot}L$$

However, the results could be explained almost as well by making K_1 the small equilibrium constant, which leads to a branched pathway:

$$M_0 + L \overset{K_0 = 2 \times 10^3}{\rightleftharpoons} M_0{\cdot}L \underset{100}{\overset{150}{\rightleftharpoons}} M_1{\cdot}L \underset{0.02}{\overset{20}{\rightleftharpoons}} M_{12}{\cdot}L$$

and

$$M_0{\cdot}L \underset{0.02}{\overset{20}{\rightleftharpoons}} M_2{\cdot}L \underset{100}{\overset{150}{\rightleftharpoons}} M_{12}{\cdot}L$$

The sequential pathway gives slightly better agreement between the calculated and measured values of k^a. Also at low temperature the amplitude of the fluorescence signal of the slow step is much smaller, which could be explained if $K_2 \ll 1$.

It is concluded that the sequential pathway for AMP-PNP binding is preferable on general grounds since the interactions of the three nucleotides AMP-PNP, ADP, and ATP with SF-1 share common features. Step 1 is fast and has a large equilibrium constant while step 2 is an order of magnitude slower and has a small equilibrium constant that decreases with temperature in each case. In interpreting the effects of the nucleotides on muscle it has been asked whether AMP-PNP is an analogue of ATP or ADP. It is evident that AMP-PNP resembles ATP in having a much larger value of K_1 than ADP, but ADP at 3 °C is similar to AMP-PNP at 20 °C and the question is probably not meaningful.

The values assigned to the rate constants for the reaction of SF-1 with ADP brings k_2 and k_{-2} into close correspondence to the rate constants of the hydrolysis step for ATP both at 20 and 3 °C (Taylor, 1977; Johnson & Taylor, 1978). It was first noted by Garland & Cheung (1979) that the occurrence of two ADP transitions lends a symmetry to the hydrolysis mechanism, which was further elucidated by Shriver & Sykes (1981) on the basis of their NMR studies and on a preliminary

report (Trybus & Taylor, 1979) of the evidence presented here. This symmetry can be made more explicit by giving the assignment of the rate constants for the complete hydrolysis cycle (0.1 M KCl, 20 °C):

$$\mathrm{ATP} + \mathrm{M_0} \underset{}{\overset{K_0 = 10^3}{\rightleftharpoons}} \mathrm{M_0{\cdot}ATP} \underset{10^{-4}}{\overset{10^3}{\rightleftharpoons}} \mathrm{M_1{\cdot}ATP} \underset{20}{\overset{100}{\rightleftharpoons}}$$

$$[\mathrm{M_{12}{\cdot}ATP},\ \mathrm{M{\cdot}ADP{\cdot}P_i}] \overset{0.05}{\longrightarrow} \mathrm{M_{12}{\cdot}ADP} \underset{100}{\overset{10}{\rightleftharpoons}} \mathrm{M_1{\cdot}ADP} \underset{10^3}{\overset{20}{\rightleftharpoons}}$$

$$\mathrm{M_0{\cdot}ADP} \underset{K_0 = 10^3}{\longrightarrow} \mathrm{M_0} + \mathrm{ADP}$$

The main difference in the transitions induced by nucleotides is the much larger equilibrium constant for the formation of M_1·ATP (or M_1·AMP-PNP), which might be explained by an electrostatic interaction of the extra charge of the γ-phosphate group. The transition to the M_{12} state appears to determine the rate of hydrolysis, which raises the question of whether hydrolysis is a further step in the mechanism. Because the hydrolysis step has a different ionic strength dependence, hydrolysis could be directly coupled to the transition to the M_{12} state, and the state in the brackets is simply M·ADP·P_i or there is an extra step in the hydrolysis mechanism and the pathway may branch.

The mechanism of the reaction of nucleotides with acto-SF-1 is complex. The dissociation of acto-SF-1 by AMP-PNP at high ionic strength gave evidence for a conformation change prior to dissociation; hence, in addition to a collision intermediate a transition to a second ternary complex must occur. The rate of dissociation of the second complex has to be slow to account for the fluorescence signal, which is faster than dissociation. The reverse reaction, the binding of SF-1–ligand to actin, showed the first intermediate to be a complex in which actin is weakly bound and thus a rapid equilibrium with free actin. Consequently, this state cannot be identical with the second ternary complex observed for ligand binding to acto-SF-1. It is concluded that a mechanism cannot be formulated with less than three acto-SF-1–ligand complexes. All of the equilibrium and rate constants cannot be uniquely determined even for a simplified scheme with only three ternary complexes, and the actual mechanism is more complex since it should include the transitions that correspond to the two first-order transitions of SF-1–ligand states as well as a branching pathway.

We will consider an oversimplified and therefore semiquantitative model. A general property of the various ternary complexes of actin, myosin, and nucleotides [ATP, ADP, AMP-PNP, ADP·P_i (the complex generated in the hydrolysis step), and ADP·vanadate] is the lower affinity of ligand or actin or both in the ternary complexes compared to the binary complexes. Since the binding sites for ligand and actin do not overlap, this property implies an interaction between sites that is transmitted by changes in conformation of myosin. The binding of actin alters the conformation of myosin so that the binding of ligand is weaker and vice versa. The interaction can be expressed quantitatively by determining the ratio of equilibrium constants of the corresponding first-order transitions for myosin and actomyosin, i.e.

$$\mathrm{M_0{\cdot}L} \overset{K_1}{\rightleftharpoons} \mathrm{M_1{\cdot}L} \qquad \mathrm{A{\cdot}M_0{}^1{\cdot}L} \overset{K_1'}{\rightleftharpoons} \mathrm{A{\cdot}M_1{}^1{\cdot}L}$$

(Highsmith, 1976, Morales & Botts, 1979). The more effectively the ligand dissociates acto-SF-1, the larger the value of K_1 (ATP > AMP-PNP > ADP). Therefore, the main interaction occurs in the transition corresponding to step 1 of the myosin scheme. K_2 is relatively small (1–10 for the three ligands) but an interaction could also occur in the second transition, leading to a further small reduction in the actin binding constant. Two-step dissociation of acto-SF-1 could be observed if the system is not fully dissociated in the first step. Marston & Taylor (1980) have reported biphasic dissociation of slow muscle acto-SF-1 with rates corresponding to k_1 and k_2 of the SF-1 kinetic scheme. We will consider a model which includes only the main interaction:

$$\begin{array}{ccccc} \mathrm{A{\cdot}M_0{}^1} + \mathrm{L} & \overset{K_0}{\rightleftharpoons} & \mathrm{A{\cdot}M_0{}^1{\cdot}L} & \overset{K_1'}{\rightleftharpoons} & \mathrm{A{\cdot}M_1{}^1{\cdot}L} \overset{K_b}{\rightleftharpoons} \mathrm{A{\cdot}M_1{}^0{\cdot}L} \\ K_a \uparrow\downarrow +\mathrm{A} & & K_a \uparrow\downarrow & & \swarrow\!\!\!\!\searrow K_c \\ \mathrm{M_0{}^0} + \mathrm{L} & \overset{K_0}{\rightleftharpoons} & \mathrm{M_0{}^0{\cdot}L} & \overset{K_1}{\rightleftharpoons} & \mathrm{M_1{}^0{\cdot}L} \end{array} \qquad (4)$$

K_a and K_c are association constants of actin with myosin–ligand complexes. The superscripts zero and one are introduced to indicate that actin binding alters the conformation of myosin. As a consequence the equilibrium constant of the first nucleotide transition is reduced ($K_1' \ll K_1$). A superscript zero indicates a state in which actin is weakly bound, which is the first intermediate formed in the reaction of actin with $M_1{}^0$·L ($K_c \ll K_a$). A second intermediate in which actin is more tightly bound (A·$M_1{}^1$·L) is formed after the initial collision complex. The apparent second-order binding constant measured by fluorescence was similar for the reaction of AMP-PNP with SF-1 and acto-SF-1; thus, the equilibrium constant for the collision intermediate (K_0) is approximately the same for both reactions [$(1–2) \times 10^3$ M^{-1}]. The transition from A·$M_1{}^1$·L is required by the relatively slow dissociation of acto-SF-1, which occurs after a faster fluorescence signal.

The association constants for the binding of ADP and AMP-PNP to acto-SF-1 determined by equilibrium binding measurements are in the range $(1–7) \times 10^3$ M^{-1} (Hofmann & Goody, 1978; Greene & Eisenberg, 1978, 1980). Since $K_{eq} = K_0(1 + K_1' + K_1'K_b)$ and $K_0 = (1–2) \times 10^3$ M^{-1} determined kinetically, it follows that K_1' and K_b are approximately equal to or less than 1. This conclusion would not be altered by including other possible ternary complexes. From the experiments on the association of $M_1{}^0$·L with actin it is inferred that k_{-b} and k_{-1}' are both large (>200 s^{-1}). The very high apparent rate constant for ligand dissociation from acto-SF-1 is partly explained by the large values of these reverse rate constants. However, values of 1 or less for K_1' and K_b mean that A·$M_0{}^1$·L could make up half of the concentration of ternary complexes at equilibrium, and in this state the bound ligand is in rapid equilibrium with free ligand. The method used to determine the rate constant of ligand dissociation by measuring the rate of ATP-induced dissociation of acto-SF-1 would probably not resolve two processes having rate constants greater than 200 s^{-1}. The maximum rate of dissociation of acto-SF-1 by ligand is $k_bK_1'/(K_1' + 1)$. The lower rate of dissociation by ADP could arise primarily from a smaller value of K_1' since K_1 for ADP is roughly 100 times smaller than K_1 for AMP-PNP and K_1' may be reduced proportionately. A unique explanation cannot be given since a further interaction involving the second nucleotide transition may be necessary to give appreciable dissociation.

It is important to note that the large reduction in equilibrium constant of the nucleotide-induced transition arises primarily from an increase in rate of the reverse reaction (k_{-1}') rather than a reduction in the rate of the forward reaction.

A complete mechanism that permits two acto–myosin states and four myosin–ligand states by including a branched pathway has eight possible ternary complexes. We have therefore restricted the discussion to a simplified scheme that still allows qualitative conclusions to be drawn for the main features of the kinetic behavior.

The studies presented here are relevant to models of muscle contraction. Models based on the kinetic scheme of actomyosin ATPase have generally assigned different orientations of the cross bridge to states defined by biochemical labels (AM·ATP, AM·ADP·P_i, AM·ADP, etc.). A recent model (Eisenberg & Greene, 1980) has proposed that the two orientations may be correlated with the strength of actin binding, and, thus, AM·ADP has a 45° orientation and AM-ATP and AM·ADP·P_i have a 90° orientation. Marston et al. (1979) have attributed a 90° orientation to AM-AMP-PNP since binding of this nucleotide reduces the tension of a rigor muscle while ADP has a much smaller effect. Although there is no direct evidence that the various nucleotide states are correlated with cross bridge orientations, it is clear that there can be no unique correlation of the biochemical labels with orientations since there are two or three states for each binary or ternary complex. Since each complex defined by a biochemical label consists of a set of intermediate states with different affinities for actin, a more reasonable hypothesis is the assignment of different orientations to each intermediate (Shriver & Sykes, 1981). Although the same set of orientation states may be present when ADP or AMP-PNP is bound to a muscle, the relative concentrations of the different orientation states in an equilibrium mixture will be different for the two nucleotides. At present the assignment of cross bridge orientations of nucleotide states has to be considered an arbitrary assumption of the particular model.

References

Bagshaw, C. R., & Trentham, D. R. (1974) *Biochem. J. 141*, 331–349.

Bagshaw, C. R., Eccleston, J. F., Trentham, D. R., Yates, D. W., & Goody, R. S. (1972) *Cold Spring Harbor Symp. Quant. Biol. 37*, 127–135.

Bagshaw, C. R., Eccleston, J. F., Eckstein, F., Goody, R. S., Gutfreund, H., & Trentham, D. R. (1974) *Biochem. J. 141*, 351–364.

Benson, S. W. (1960) *The Foundation of Chemical Kinetics*, McGraw-Hill, New York.

Chock, S. P. (1979) *J. Biol. Chem. 254*, 3244–3248.

Chock, S. P., Chock, P. B., & Eisenberg, E. (1979) *J. Biol. Chem. 254*, 3236–3243.

Eisenberg, E., & Greene, L. E. (1980) *Annu. Rev. Physiol. 42*, 293–309.

Garland, F., & Cheung, H. C. (1979) *Biochemistry 18*, 5281–5289.

Greene, L. E., & Eisenberg, E. (1978) *Proc. Natl. Acad. Sci. U.S.A. 75*, 54–58.

Greene, L. E., & Eisenberg, E. (1980) *J. Biol. Chem. 255*, 543–548.

Gutfreund, H. (1975) *Prog. Biophys. Mol. Biol. 29*, 161–195.

Highsmith, S. (1976) *J. Biol. Chem. 251*, 6170–6172.

Hofmann, W., & Goody, R. S. (1978) *FEBS Lett. 89*, 169–172.

Johnson, K. A., & Taylor, E. W. (1978) *Biochemistry 17*, 3432–3442.

Koretz, J. F., & Taylor, E. W. (1975) *J. Biol. Chem. 250*, 6344–6350.

Marsh, D. J., deBruin, S. H., & Gratzer, W. B. (1977) *Biochemistry 16*, 1738–1742.

Marston, S. B., & Taylor, E. W. (1980) *J. Mol. Biol. 139*, 573–600.

Marston, S. B., Tregear, R. T., Rodger, C. D., & Clarke, M. L. (1979) *J. Mol. Biol. 128*, 111–126.

Morales, M. F., & Botts, J. (1979) *Proc. Natl. Acad. Sci. U.S.A. 76*, 3857–3859.

Shriver, J. W., & Sykes, B. D. (1981) *Biochemistry 20*, 2004–2012.

Sleep, J. A., Trybus, K. M., Johnson, K. A., & Taylor, E. W. (1981) *J. Muscle Res. Cell Motil.* (in press).

Taylor, E. W. (1977) *Biochemistry 16*, 732–740.

Taylor, R. S., & Weeds, A. G. (1976) *Biochem. J. 159*, 301–315.

Trybus, K. M., & Taylor, E. W. (1979) *Biophys. J. 25*, M-AM-D11.

Weeds, A. G., & Taylor, R. S. (1975) *Nature (London) 257*, 54–56.

White, H. D. (1977) *Biophys. J. 17*, 40a.